The stability of binary charged colloidal crystals

Wan Y. Shih, Wei-Heng Shih, and Ilhan A. Aksay
Department of Materials Science and Engineering, and Advanced Materials Technology Program, Washington Technology Center, University of Washington, FB-10, Seattle, Washington 98195

(Received 15 November 1988, accepted 6 December 1988)

The stability of a binary disordered substitutional colloidal crystal has been examined against the formation of a colloidal liquid. Phase diagrams are constructed by comparing the free energy of the liquid phase to that of the solid phases. The calculations show that the freezing density has a maximum as a function of the number fraction. The maximum in the freezing density becomes more pronounced when the particle diameter ratio differs more from unity. If the particles have very different diameters, the binary colloidal crystals are unstable against the colloidal fluid. The freezing density rises almost vertically when the number fraction differs from 0 or 1 by less than 6%. The pronounced stability of the liquid phase for particles with more different sizes may explain the formation of colloidal glasses as opposed to the formation of disordered substitutional colloidal crystals with particles of more similar diameters. The Hume–Rothery rule for a binary metallic alloy also applies to a binary charged colloid if the diameter ratio is taken from the diameters of the effective hard spheres which are determined by the interparticle interactions but not those of the bare particles.

INTRODUCTION

Partly because of the practical importance of the study of colloidal systems to modern colloidal processing, and partly because of the availability of uniformly sized particles which make many studies possible, interest has increased in the study of colloidal systems. A charged colloidal system at low densities is very much like a liquid metal. The particles constitute the "ions" and the ions (including the counter ions dissolved from the particles and the stray ions in the solution) constitute the "electrons." The difference is, of course, that the size and the charge of a colloidal particle is about 1000 times larger than those of its atomic counterpart. Of particular interest are uniformly sized particles which can freeze into colloidal crystals when a high enough density is reached.[1] Face-centered-cubic (fcc) and body-centered-cubic (bcc) are the two stable crystalline structures.[2]

When particles of two different sizes are mixed together, the situation becomes more complicated because there are now two more parameters to change, namely, the particle diameter ratio and the number fraction. Experimentally, it is found that when the diameters of the two species are somewhat similar, one forms a homogeneous crystalline solid solution for all number fractions which is characterized both by a finite shear modulus and by Bragg diffraction, similar to a disordered substitutional alloy. The mixtures of polystyrene spheres of radii 545 and 445 Å are such examples.[3] The diameter ratio in these mixtures is about 0.817.

When the diameter ratio of the two species differs more from unity, one may form a colloidal glass or a crystalline colloidal compound depending on how long the system is allowed to reach equilibrium. For example, mixtures of polystyrene spheres[3,4] of radii 1100 and 545 Å have been found to form one homogeneous disordered solid (colloidal glass) characterized by a finite shear modulus but no Bragg diffraction when the number fraction is more than 5% from either end of the phase diagram; crystallinity is retained in the small regions ($< 5\%$) near the pure cases. Similar disordered colloidal solids can also be formed with larger colloidal particles. Liniger and Raj[5] reported that polystyrene spheres of 5 and 7 μ diameters formed disordered solids when the volume fraction of the 7 μ particles is from 10% to 90% and ordered solids otherwise in an air-water interface. The diameter ratio for these mixtures is about 0.7. However, for particles in the micron size, the order–disorder transition cannot be studied with a further decreased diameter ratio because of differential settling.[5]

The formation of colloidal glasses was observed on a shorter time scale. If a colloidal mixture is allowed to equilibrate fully, a colloidal compound may be formed that has a complex crystalline structure similar to that of an intermetallic compound. For example, the above mentioned colloidal glasses formed with polystyrene particles of radii 1100 and 545 Å were reported to transform into colloidal compounds a year or so later.[3,4] Under suitable conditions, Hachisu and Yoshimura[6,7] were able to identify four different compound structures ($NaZn_{13}$, AlB_2, $CaCu_5$, and $MgCu_2$) with binary polystyrene spheres with individual particle diameters ranging from 2000 to 8000 Å. The exact crystalline structure depends on a number of parameters such as the particle diameter ratio, the number fraction, and the number densities. However, the equilibration of a colloidal mixture may take years, as mentioned in Refs. 3 and 4. Equilibrium is thus not always reachable within the laboratory time frame. Instead, what one often finds in a colloidal mixture may be only short-time phenomena and may be metastable. In light of this, we feel it is probably of more practical importance to discuss the "metastable" phenomena, i.e., the formation of a colloidal glass, than to discuss the stability of various colloidal compounds. Although the formation of various colloidal compounds at equilibrium is also interesting, we will not consider it in this paper.

For the atomic analog of a binary colloid, namely a bina-

 0021-9606/89/084506-07$02.10

ry metallic system, the Hume-Rothery rule[8] says that a substitutional alloy can not be formed when the diameters of the two atomic species differ more than 15%. Furthermore, the immiscibility of the two species in the crystalline form is usually accompanied by the formation of deep eutectics,[9] i.e., with fractional concentrations at which the liquid is stable to an especially low temperature. It is also known that the glass forming trend in metallic alloys is often related to deep eutectics.[10]

The purpose of this paper is to establish binary colloidal phase diagrams which show the "stability" regions of the colloidal substitutional alloys relative to the colloidal liquid. From the stability of the crystalline substitutional alloys, we can address the miscibility in binary colloidal crystals. By correlating with the deep eutectics in the phase diagrams, we will be able to address the question concerning colloidal glass forming. However, we must point out that the binary colloidal phase diagrams we establish in this paper may not be those at equilibrium since we do not consider the formation of various compounds. Nevertheless, the "metastable" phase diagrams we calculate here are still meaningful since in the laboratory time frame many of the colloidal systems are not at equilibrium.

The phase boundaries between the liquid and the disordered substitutional colloidal alloys will be constructed by directly comparing the free energies of the liquid to those of the solids (for which we have considered both fcc and bcc disordered substitutional alloys). The "stable" phase will be the one with the lowest free energy. In general, one should draw a common tangent in order to establish the two-phase regions in the phase diagrams. However, neither the experiment nor the theory is accurate enough to allow this procedure. The free energies of various phases are calculated by means of a variational principle based on the Gibbs–Bogolyubov inequality. Einstein oscillators are used as the reference system of the solid phases, and a binary hard sphere mixture is used as the reference system for the liquid. This approach has been successfully applied to calculate the phase diagrams of monodisperse charged colloidal particles.[2]

We now turn to the body of the paper. Section II briefly describes the formalism. Section III gives the results and discussions, while some concluding remarks are given in Sec. IV.

MODEL

We consider a binary aqueous suspension of N_1 particles of radius a_1, charge Z_1, and N_2 particles of radius a_2, charge Z_2 with volume Ω. In the absence of added electrolytes, there will be $N_1Z_1 + N_2Z_2$ counter ions (H_3O^+ or OH^- depending on the system) in solutions to neutralize the charges on the colloidal particles. If the number density of the colloidal particles is not too high or the temperature is not too low, the effective interactions between the colloidal particles can be adequately treated within the Debye–Hückel approximation. In MKSA units, the interaction takes the form

$$U(r_{ij}) = \frac{Z_iZ_je^2}{4\pi\epsilon_0\epsilon r_{ij}}\left[\frac{e^{qa_i}}{1+qa_i}\right]\left[\frac{e^{qa_j}}{1+qa_j}\right]e^{-qr_{ij}}, \quad (2.1)$$

Here r_{ij} is the separation between the centers of particle i and particle j, ϵ is the static dieletric constant of water, ϵ_0 is the permittivity of free space, e is the electronic charge, and q is the inverse screening length which satisfies

$$q^2 = \frac{e^2}{\epsilon_0\epsilon k_BT}\sum_i n_i(z_i^2), \quad (2.2)$$

where k_B is the Boltzmann constant, T is the absolute temperature, z_i and n_i are the charge and the number density of the ith species of ions, respectively. The term in the brackets of Eq. (2.1) is the size correction which takes into account the fact that part of the volume of the suspension is not available for screening due to the finite sizes of the colloidal particles. This correction is important in determining the melting behavior of the colloidal suspensions.[11]

When the colloidal suspension is at equilibrium, its thermodynamic properties are determined by the Helmholtz free energy $F = E - TS$, where E is the total energy and S is the entropy. For a system of particles interacting via the potential Eq. (2.1), the free energy per particle takes the following form:

$$F = \frac{1}{2N}\sum_{\substack{i,j\\ i\neq j}}^{N}\frac{Z_iZ_je^2}{4\pi\epsilon_0\epsilon}\left(\frac{e^{qa_i}}{1+qa_i}\right)\left(\frac{e^{qa_j}}{1+qa_j}\right) \times\left\langle\frac{1}{|\mathbf{r}_i-\mathbf{r}_j|}e^{-q|\mathbf{r}_i-\mathbf{r}_j|}\right\rangle + E_{\text{kin}} - TS, \quad (2.3)$$

where E_{kin} and S are the kinetic energy and the entropy per particle, $N = N_1 + N_2$ is the total number of particles in the system, $\langle\ \rangle$ denotes the thermal average over the canonical ensemble, and $\mathbf{r}_i$ is the position of particle i. Equation (2.3) includes only the part of the free energy that depends on the arrangement of the particles. These are the terms that are relevant in determining the structure of the colloidal suspension.

The free energy can be obtained from Eq. (2.3) by the use of a variational principle based on the Gibbs–Bogolyubov inequality which states as follows:

$$F \leqslant F_0 + \langle U - U_0\rangle_0 \equiv F', \quad (2.4)$$

where F_0 is the free energy of the reference system and $\langle U - U_0\rangle$ is the potential energy difference of the system of interest and the reference system. Since F is upper bounded by F', we can then approximate F to be the minimum of F' with respect to the appropriate variables, that is, $F \simeq F'(x_0,y_0)$ and

$$\left.\frac{\partial F'(x,y)}{\partial x}\right|_{x=x_0} = 0 \text{ and } \left.\frac{\partial F'(x,y)}{\partial y}\right|_{y=y_0} = 0, \quad (2.5)$$

where x and y are the appropriate variables. In the present calculation, we use Einstein oscillators as the reference system for the solid and binary hard sphere fluid as the reference system for the liquid. This procedure has been successfully applied for the monodisperse colloidal suspensions[2] and the intermetallic alloys.[12] It is expected to work well in the present case.

Solid

It is convenient to choose an ensemble of Einstein oscillators to define the reference system: each particle of type 1

or 2 oscillates about a lattice point independently in a potential well with a frequency ω_1 and ω_2. In terms of the Einstein temperature $\theta_i = \hbar\omega_i/k_B\,(i=1,2)$ and with random alloy approximation, we may write the right-hand side of Eq. (2.4) as

$$F = E_{\rm kin} - TS + \frac{1}{2}\sum_{\mathbf{R}\neq 0}\sum_{i,j=1}^{2}\frac{e^2}{4\pi\epsilon_0\epsilon}x_iZ_ix_jZ_j\left(\frac{e^{qa_i}}{1+qa_i}\right)\left(\frac{e^{qa_j}}{1+qa_j}\right)f_{ij}(|\mathbf{R}|)$$
$$-\frac{e^2q}{8\pi\epsilon\epsilon_0}\left(x_1Z_1^2\frac{e^{2qa_1}}{(1+qa_1)^2}+x_2Z_2^2\frac{e^{2qa_2}}{(1+qa_2)^2}\right)-\frac{ne^2}{2\epsilon\epsilon_0q^2}\left[x_1Z_1\left(\frac{e^{qa_1}}{(1+qa_1)}\right)+x_2Z_2\left(\frac{e^{qa_2}}{(1+qa_2)}\right)\right]^2 \quad (2.6)$$

in which $x_i = N_i/N$, for $i=1,2$, $\mathbf{R}$ is the lattice vector, N/Ω is the number density of the colloidal particles, and

$$E_{\rm kin} = \frac{3}{2}k_BT, \quad (2.7)$$

$$TS = 3k_BT\sum_{i=1}^{2}x_i[1-\ln(\theta_i/T)], \quad (2.8)$$

and

$$f_{ij}(r) = \frac{1}{2r}e^{(W_i+W_j)q^2}\left[e^{-qr}\left(1-\mathrm{erf}\left[(W_i+W_i)^{1/2}q - \frac{r}{2(W_i+W_j)^{1/2}}\right]\right) - e^{qr}\left(1-\mathrm{erf}(W_i+W_j)^{1/2}q+\frac{r}{2(W_i+W_j)^{1/2}}\right)\right], \quad (2.9)$$

where erf is the error function

$$\mathrm{erf}(x) = \frac{2}{(\pi)^{1/2}}\int_0^x e^{-y^2}\,dy, \quad (2.10)$$

and $6W_i$ is the mean square displacement which takes the following form:

$$W_i = \frac{\hbar^2\coth(\theta_i/2T)}{4M_ik_B\theta_i} \quad i=1,2, \quad (2.11)$$

in which M_i is the mass of the particles of type i. Note that the anharmonic effect has been taken into account in Eq. (2.9). The right-hand side of Eq. (2.6) may then be minimized with respect to θ_1 and θ_2 to give the upper bound of the structure-dependent part of the free energy of the colloidal substitutional alloys. In the actual calculations, $r/2(W_i+W_j)^{1/2} \pm (W_i+W_j)^{1/2}q$ is much larger than unity and Eq. (2.9) reduces to

$$f_{ij}(r) \simeq e^{(W_i+W_j)q^2}\frac{e^{-qr}}{r}. \quad (2.12)$$

Liquid

For the reference system of the liquid phase we consider a binary hard sphere fluid where particles are interacting via the hard sphere potential,

$$U_0(r_{ij}) = \begin{cases}\infty & r_{ij}<\sigma_{ij}\\ 0 & r_{ij}\geqslant\sigma_{ij}\end{cases} \quad (2.13)$$

in which $\sigma_{ij} = (\sigma_i+\sigma_j)/2$, where σ_i, the effective hard sphere diameter of particle i, is not, in general, equal to a_i, the actual diameter of a type-i particle. With this choice of the hard-sphere mixture as the reference system, the right-hand side of Eq. (2.6) can be written as

$$F = F_{hs}(\sigma_1,\sigma_2,x_1) - \frac{e^2q}{8\pi\epsilon\epsilon_0}\left(x_1Z_1^2\frac{e^{2qa_1}}{(1+qa_1)^2}+x_2Z_2^2\frac{e^{2qa_2}}{(1+qa_2)^2}\right) + \frac{ne^2}{8\pi\epsilon\epsilon_0}\sum_{i,j=1}^{2}\int dr\,4\pi r^2\frac{e^{-qr}}{r}\left(\frac{e^{qa_i}}{1+qa_i}\right)\times\left(\frac{e^{qa_j}}{1+qa_j}\right)[g_{ij}(r)-1]\,x_ix_jZ_iZ_j, \quad (2.14)$$

where $F_{\rm hs}$ is the Helmholtz free energy of a hard-sphere mixture of diameter σ_1 and σ_2. The functions $g_{ij}(r)$ are the appropriate pair distribution functions for the reference systems, normalized to equal unity in the limit of large r. The terms involving $g_{ij}(r)$ can be evaluated analytically in the Percus–Yevick approximation for arbitrary ratios of the hard sphere diameters; explicit expressions of the terms involving $g_{ij}(r)$ have been given by Lebowitz.[13] These may be combined with the approximate analytic formulas given by Umar *et al.*[14] for the free energy $F_{\rm hs}(\theta_1,\sigma_2,x_1)$ of the hard sphere mixture (based on the equation of state derived from the Percus–Yevick hard-sphere partition function) to give a close-form expression for the structure-dependent part of the right-hand side of Eq. (2.6). This part may then be minimized with respect to σ_1 and σ_2 to obtain the upper bound of the structure-dependent part of the free energy of the binary colloidal liquids

RESULTS AND DISCUSSIONS

To test our theory for a binary colloid, we first calculate the freezing densities for the colloidal mixtures that were reported experimentally in Refs. 3 and 4. The resulting freezing densities as a function of the number fraction of the large particles are plotted in Figs. 1(a) and 1(b) where D stands for the total number density of the colloidal mixture and $x = x_1 = N_1/(N_1+N_2)$ stands for the number fraction of the large spheres. Figure 1(a) is for the case where $Z_1 = 300$, $a_1 = 545$ Å and $Z_2 = 245$, $a_2 = 445$ Å. Figure 1(b) is for the case where $Z_1 = 600$, $a_1 = 1100$ Å and $Z_2 = 300$, $a_2 = 545$ Å. These values were taken from Ref. 3. Figure 1(a) shows that the mixtures of 545 and 445 Å particles form disordered substitutional fcc alloy at higher densities for all values of x,

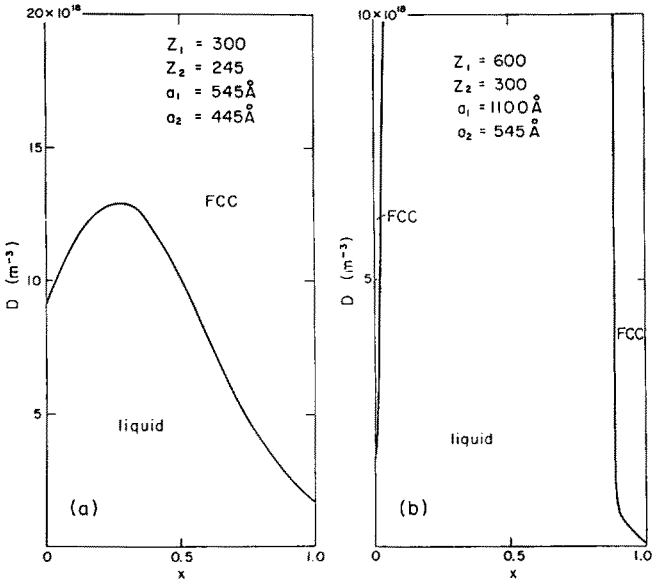

FIG. 1. D–x phase diagrams of binary colloidal particles where D is the total number density and x is the number fraction of the large particles.

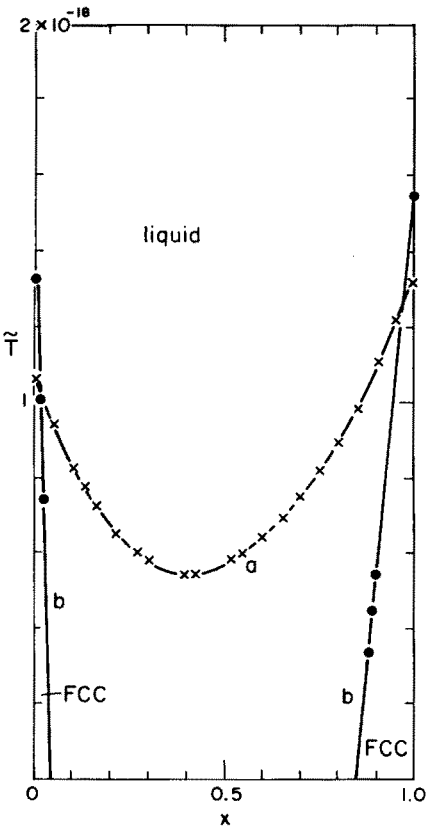

FIG. 2. $\tilde{T}-x$ phase diagrams of the binary colloidal particles in Fig. 1. $\tilde{T}$ is the effective temperature as defined in the text, and x is as in Fig. 1.

in qualitative agreement with the observation in Ref. 3. The actual diameter ratio is about 0.817 in these mixtures. However, the diameter ratio of the effective hard spheres is about 0.92. Note that there is a maximum in the freezing-density-vs-x curve indicating that the fluid phase can remain stable up to a higher density in the mixture than in the pure cases. We will show below that this maximum in the freezing density in the D–x plane actually corresponds to an azeotropic or a eutectic in the T–x phase diagram.

In Fig. 1(b), it is shown that mixtures of 1100 and 545 Å particles form no substitutional alloys in most of the phase space except for very small regions near $x=0$ and $x=1$ where the face-center-cubic (fcc) substitutional alloy is still stable. The small crystalline regions in Fig. 1(b) is in agreement with Ref. 3. The actual diameter ratio for these mixtures is about 0.5 while the diameter ratio of the effective hard spheres is about 0.75, both of which are smaller than those of the mixtures of Fig. 1(a).

The disappearance of the crystalline phase in Fig. 1(b) for an intermediate value of x up to very high densities signals a very pronounced maximum in the freezing densities as a function of x (or a very deep eutectic in the T–x phase diagram). Thus, the mixtures of 1100 and 545 Å particles should be more likely to form colloidal glasses than the mixtures of 545 and 445 Å particles. Indeed, this was the experimental observation.

To illustrate that a maximum in the freezing densities is equivalent to a minimum in the freezing temperature, we define an effective temperature $\tilde{T}=k_BT/(Z^2e^2/4\pi\epsilon_0\epsilon a_s)$ where $Z=x_1Z_1+x_2Z_2$ is the average charge and $a_s=D^{-1/3}$ is the average nearest distance between particles. In Fig. 2 we plot the effective freezing temperature as a function of x for the mixtures of 545 and 445 Å particles in curve (a) and that for the mixtures of 1100 and 545 Å particles in curve (b). Curve (a) indeed shows a minimum in the effective freezing temperature which reflects the maximum in the freezing density. In curve (b), again, the crystalline phase is unstable in most of the $\tilde{T}-x$ phase space except for small regions near $x=0$ and $x=1$ just as in the D–x phase diagram. The instability of the crystalline phase indicates a very deep minimum in the freezing temperature. In fact, the extrapolation of curve (b) shows that fluid mixtures are stable down to zero temperature for most values of x. Notice that the location of the minimum freezing temperature in Fig. 2(a), which is near $x=0.4$, is not the same as that of the maximum freezing density in Fig. 1(a), which is near $x=0.3$. The reason is that our $\tilde{T}$ is only approximate. If we were to use a different definition, such as $\tilde{T}=k_BT/E_{\rm ave}$, where $E_{\rm ave}$ is the average energy per particle, we would have a more accurate representation of the effective temperature and hence a better agreement between Figs. 1(a) and 2(a) as to where the maximum freezing density and the minimum freezing temperature occur. Nonetheless, Figs. 1(a)–1(b) and Figs. 2(a)–2(b) show the correspondence between the freezing density and the effective freezing temperature. To relate the minima in the freezing temperatures that we have obtained to eutectics requires calculations of the miscibility at low temperatures (or high densities) for a eutectic is usually associated with not only an especially low melting point, but also with immiscibility in the solid phase. Shih and Stroud[15] have studied the miscibility of these colloidal mixtures in the liquid form and have shown that the mixtures do indeed phase separate at high densities. Phase separation begins at around $D=13\times10^{18}$ m^{-3} for the mixtures of particles of 445 and 545 Å, which is near the maximum of the

freezing density in Fig. 1(a). For mixtures of particles of 545 and 1100 Å, phase separation begins at around $D = 1.6\times10^{18}\ \mathrm{m}^{-3}$, which is between the freezing densities of the pure cases. Although their predictions for phase separation are for liquid mixtures, the results are still appreciable when one considers phase separation between two solid phases (or between the solid and the liquid phases). The reason is that the excess free energy comes mostly from the mixing of the counter ions in the solutions because the ions outnumber the particles.[15] The structural part of the free energy is only a small portion of the total free energy. Thus, our maxima of the freezing densities (or minima in the freezing temperature) do relate to a eutectic, and the depth of the extrema does reflect the difficulty of mixing the particles. Comparing the diameter ratio for the mixtures of curves (a) and (b), one finds an analog of the Hume–Rothery rule in a binary colloid. However, one should note that the 15% difference in diameters for the miscibility margin relates more closely to the effective hard-sphere diameter ratio, which is 0.92 for curve (a) and 0.75 for curve (b), than to the actual particle diameter ratio, which is 0.817 for (a) and 0.5 for (b). This is reasonable since the atomic diameters used in the Hume–Rothery rule are also effective hard sphere diameters. Note that the interaction between these highly charged colloidal particles is repulsive and long ranged. Thus, what influences the interparticle arrangement would be the effective hard-sphere diameters which are determined by the range of the interparticle interactions but not by the actual particle diameters. This point may also be seen when one considers the low densities (typically a few volume per cent) of these colloidal crystals where the average nearest particle distance is about four or five times the actual particle diameters.

To illustrate this point more clearly, we plot the freezing densities of mixtures with actual particle diameter ratios ranging from 0.9 to 0.7 in Figs. 3(a)–3(d). For all the cases shown, the large particles have a radius $a_1 = 545$ Å and a surface charge $Z_1 = 300$. For the small particles, we use the linear-diameter-charge relationship proposed by Pincus[15,16] to determine the charge for particles of a given size: $a_2 = 491$ Å, $Z_2 = 270$ in Fig. 3(a); $a_2 = 445$ Å, $Z_2 = 245$ in Fig. 3(b); $a_2 = 409$ Å, $Z_2 = 225$ in Fig. 3(c); and $a_2 = 382$ Å, $Z_2 = 210$ in Fig. 3(d). The actual particle diameter ratio is 0.9 in Fig. 3(a), 0.817 in Fig. 3(b), 0.75 in Fig. 3(c) and 0.7 in Fig. 3(d), while the diameter ratio of the effective hard spheres is 0.96 in Fig. 3(a), 0.92 in Fig. 3(b), 0.89 in Fig. 3(c), and 0.86 in Fig. 3(d). One can see that as the particle diameter ratio decreased more from unity, the freezing curve in the D–x phase diagram began to show a maximum with respect to x. Note that there is indeed a weak maximum which occurs near $x = 0$ in curve (a) which may be better seen from the minimum in $\tilde{T} - x$ plane when we plot the effective freezing temperature in Fig. 4. The maximum becomes more pronounced as the diameter ratio is progressively decreased. As a result, the disordered crystalline alloy phase shrinks to small regions near $x = 0$ and $x = 1$ for the small particle diameter ratio as is shown in Figs. 3 (c)–3(d) and in Fig. 1(a). Note that the solubility of small spheres in the crystals of large spheres is always larger than the solubility of large spheres in the crystals of small spheres. This feature is also seen in the recent density-functional calculations of binary hard spheres.[17] Also note that the solid–liquid phase boundaries in Fig. 3(d) almost open up vertically at the high densities and the effective hard-sphere diameter ratio is 0.86 in this case. When the effective hard sphere diameter ratio decreases further, the solid–liquid phase boundaries rise even more sharply from $x = 0$ and $x = 1$, as shown in Fig. 1(a), where the effective hard sphere diameter ratio is 0.7. This suggests that the Hume–Rothery rule may be used in binary colloids only that the effective hard sphere diameters must be used for the miscibility criterion instead of the bare particle diameters. We also plot the effective freezing densities for all four cases in Fig. 4. As the particle diameter ratio becomes smaller, the minimum freezing temperature becomes deeper. Again, the locations of the maxima in Figs. 3(a)–3(d) are not the same as those of the minima in Figs. 4(a)–4(d), as we have explained above.

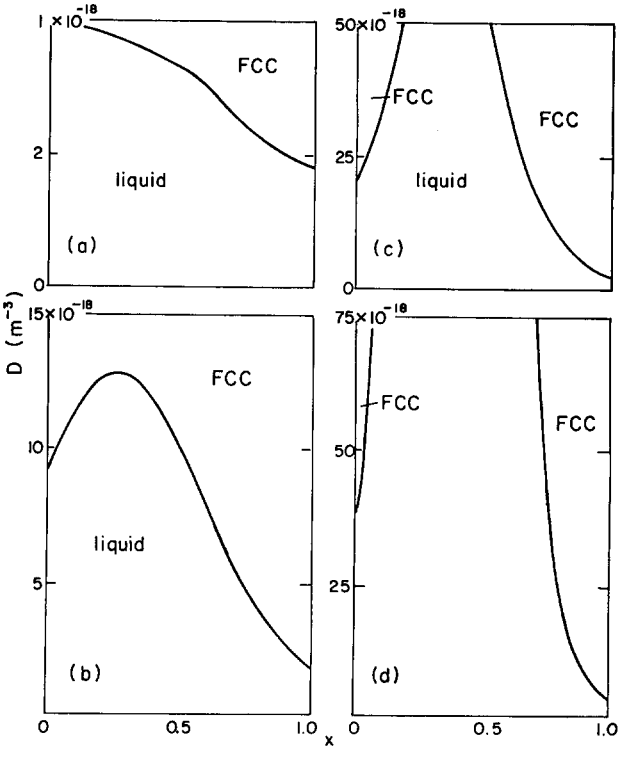

FIG. 3. D–x phase diagrams of binary colloidal particles with diameter ratio ranging 0.9 – 0.7. $a_1 = 545$ Å, $Z_1 = 300$ for all cases, while $a_2 = 491$ Å, $Z_2 = 270$ in (a); $a_2 = 445$ Å, $Z_2 = 245$ in (b); $a_2 = 409$ Å, $Z_2 = 225$ in (c); and $a_2 = 382$ Å, $Z_2 = 210$ in (d).

Finally, we show in Fig. 5 the effect of adding salt for a mixture of particles of diameter $a_1 = 545$ Å, charge $Z_1 = 300$ and particles of diameter $a_2 = 445$ Å, charge $Z_2 = 245$. Curve (a) is for the case of no added salt, curve (b) is for the case of 10 μM salt and curve (c) is for 20 μM salt. Note that adding salt has the effect of decreasing the interparticle repulsion by screening and thus increasing the freezing density. Moreover, the shortened screening length makes the particles more like hard spheres. As a result, the effective hard sphere diameter ratio should move closer towards the bare particle diameter ratio. Indeed, this is the case; the effective hard sphere diameter ratio is 0.91 with 20

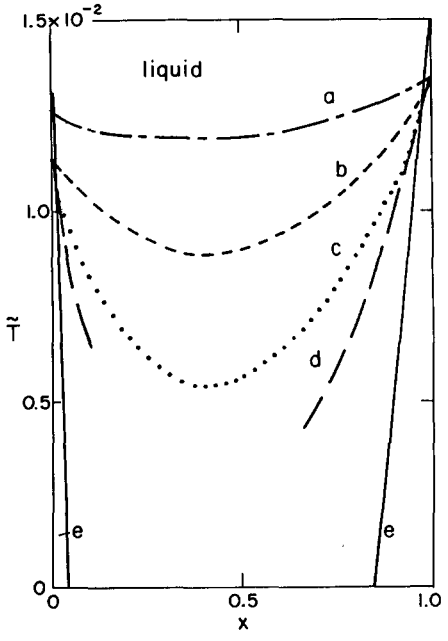

FIG. 4. $\tilde{T} - x$ phase diagrams of binary colloidal particles. Curves (a)–(d) correspond to the freezing temperatures of Figs. 3(a)–3(d) while (e) corresponds to Fig. 1(b).

μM salt as compared to 0.92 without salt where the bare particle diameter ratio is 0.817. In these mixtures, the diameter ratio of the effective hard spheres is larger than that of the bare particles. Thus, adding salt to change the diameter ratio of the effective hard spheres towards that of the bare particles enhances the maximum of the freezing curve in the D–x plane (minimum in the $T - x$ plane).

CONCLUDING REMARKS

We have determined the boundaries between the liquid phase and the disordered substitutional crystalline alloys for binary colloids by comparing the free energies of both the liquid and the solid phases. The free energies have been calculated variationally using the Gibbs–Bugolyubov inequality. Einstein oscillators are the reference system for the solids; hard-sphere mixtures are the reference system for the liquids. We have shown the following: (1) For binary charged colloids, the freezing density as a function of the number fraction has a maximum. The maximum freezing density occurs in small-particle rich mixtures and the maximum freezing density increases sharply with decreasing particle diameter ratio. (2) When the effective hard sphere diameter ratio is about 0.86~0.85, the solid–liquid boundaries rise almost vertically; the liquid phase is stable in most of the phase space except for small regions near the pure cases. (3) When the effective hard sphere diameters are used for the criterion, we have shown that the Hume-Rothery rule for the stability of the atomic substitutional alloys can also apply to binary charged colloids. (4) A maximum in freezing densities is equivalent to a minimum in freezing temperatures, i.e., an azeotropic or a eutectic. (5) Adding salt can enhance the maximum in the freezing density. (6) Finally, the pronounced stability of the liquid phase, i.e., the maximum in the freezing density in a colloidal mixture reflects the immiscibility at high densities (or low temperatures) just as it does in a binary metallic alloy. The glass formation observed experimentally corresponds to a deep minimum in the freezing temperatures (or pronounced freezing densities) in our calculation. The fact that the fluid phase can be stable up to an especially high density in a binary colloidal suspension can be helpful in colloidal processing where a high green-compact density is desired. A suspension of bimodal particle distribution may be used to achieve that goal. Indeed, this has been observed. Han *et al.*[18] have obtained a maximum in the green-body density (higher than those of the pure cases) when using a bimodal suspension. Another measurement that can reflect the maximum in the freezing densities we have discussed in this paper is the viscosity of the colloidal suspensions. The viscosity of the bimodal colloidal suspension may be found to have a minimum as a function of the number fraction at fixed particle number density (or total volume fraction). This has also been observed.[19]

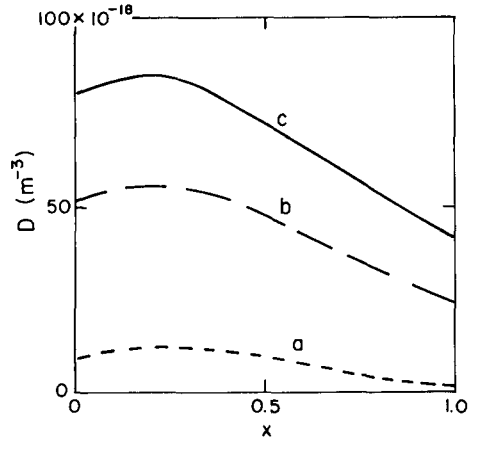

FIG. 5. D–x phase diagrams of binary colloidal particles where $a_1 = 545$, $Z_1 = 300$ and $a_2 = 445$, $Z_2 = 245$. Curve (a) is the freezing density without adding salt, (b) is that with 10 μM salt, and (c) is with 20 μM salt.

ACKNOWLEDGMENTS

The work was supported by the Air Force Office of Scientfic Research (AFOSR) and the Defense Advanced Research Projects Agency (DARPA) of the U.S. Department of Defense and was monitored by the AFOSR under Grant No. AFOSR-87-0114.

[1]For a review of general properties of colloidal crystals and liquids, see P. Pieranski, Contemp. Phys. **24**, 25 (1983).
[2]W. Y. Shih, I. A. Aksay, and R. Kikuchi, J. Chem. Phys. **86**, 5127 (1987).
[3]P. M. Chaikin and P. A. Pincus (unpublished).
[4]H. M. Lindsay and P. M. Chaikin, J. Chem. Phys. **76**, 3774 (1982).
[5]E. Liniger and R. Raj, J. Am. Ceram. Soc. **70**, 843 (1987).
[6]S. Hachisu and S. Yoshimura, Nature **283**, 188 (1980).
[7]S. Yoshimura and S. Hachisu, J. Phys. Colloq. C3, **46**, 115 (1987).
[8]W. Hume-Rothery, R. E. Smallman, and C. W. Haworth, *The Structure of Metals and Alloys* (Metals and Metallurgy Trust, London, 1969).
[9]For example, see M. Hansen, *Constitution of Binary Alloys* (McGraw-Hill, New York, 1958).
[10]For more general information on structural properties of metallic glasses, see D. Turnbull, J. Phys. (Paris) **35**, C4-1 (1974).

[11]W.-H. Shih and D. Stroud, J. Chem. Phys. **79**, 6254 (1983).
[12]W. Y. Shih and D. Stroud, Phys. Rev. B **32**, 7779 (1985); *ibid*, 7785 (1985).
[13]J. Lebowitz, Phys. Rev. A **133**, 895 (1964).
[14]I. H. Umar, A. Meyer, M. Watabe, and W. H. Young, J. Phys. F **4**, 1691 (1974).
[15]P. Pincus, Invited Paper at March Meeting of the American Physical Society, Los Angeles, California, 1983 (unpublished).
[16]W.-H. Shih and D. Stroud, J. Chem. Phys. **80**, 4429 (1984).
[17]J. L. Barrat, M. Baus, and J. P. Hansen, Phys. Rev. Lett. **56**, 1063 (1986).
[18]C. Han, I. A. Aksay, and O. J. Whittemore, in *Advances in Materials Characterization II*, edited by R. L. Snyder, R. A. Condrate, P. F. Johnson (Plenum, New York, 1985), p. 339.
[19]K. P. Darcovich and I. A. Aksay (unpublished).